Identification of *Caenorhabditis elegans* Genes Required for Neuronal Differentiation and Migration

Wayne C. Forrester,* Elliot Perens,* Jennifer A. Zallen† and Gian Garriga*

**Department of Molecular and Cell Biology, University of California, Berkeley, California 94720 and*
†Department of Anatomy, University of California, San Francisco, California 94143

Manuscript received June 26, 1997
Accepted for publication September 8, 1997

ABSTRACT

To understand the mechanisms that guide migrating cells, we have been studying the embryonic migrations of the *C. elegans* canal-associated neurons (CANs). Here, we describe two screens used to identify genes involved in CAN migration. First, we screened for mutants that died as clear larvae (Clr) or had withered tails (Wit), phenotypes displayed by animals lacking normal CAN function. Second, we screened directly for mutants with missing or misplaced CANs. We isolated and characterized 30 mutants that defined 14 genes necessary for CAN migration. We found that one of the genes, *ceh-10*, specifies CAN fate. *ceh-10* had been defined molecularly as encoding a homeodomain protein expressed in the CANs. Mutations that reduce *ceh-10* function result in Wit animals with CANs that are partially defective in their migrations. Mutations that eliminate *ceh-10* function result in Clr animals with CANs that fail to migrate or express CEH-23, a CAN differentiation marker. Null mutants also fail to express CEH-10, suggesting that CEH-10 regulates its own expression. Finally, we found that *ceh-10* is necessary for the differentiation of AIY and RMED, two additional cells that express CEH-10.

DURING nervous system development, neurons migrate, extend growth cones to their targets, synapse with other cells, and express specific neurotransmitters. To achieve its final pattern of connectivity, a neuron must express proteins that regulate cell migration, axonal outgrowth, synapse formation and neurotransmitter expression. We have been particularly interested in understanding the mechanisms that regulate cell migration and axonal outgrowth.

Cell migration and axonal outgrowth are complicated processes that are likely to require many proteins. Extracellular matrix molecules such as laminin are thought to provide a permissive environment for cell motility (Lander 1989). Additional extracellular matrix molecules such as the UNC-6/netrins play instructive roles, guiding migrations along the dorsoventral axis of nematodes, flies and vertebrates (Serafini *et al.* 1994, 1996; Harris *et al.* 1996; Mitchell *et al.* 1996; Wadsworth *et al.* 1996). Signals from extracellular guidance cues are mediated by receptors. For example, the UNC-5 and UNC-40/DCC netrin receptors appear to repel and attract growth cones, respectively (Leung-Hagesteijn *et al.* 1992; Chan *et al.* 1996; Keino *et al.* 1996; Kolodziej *et al.* 1996; Ackerman *et al.* 1997; Fazeli *et al.* 1997; Leonardo *et al.* 1997). Signals are integrated by intracellular signaling molecules. Members of the Rho family of Ras-like small GTPases, CDC-42, Rac and Rho, are intracellular signaling molecules that apparently act on discrete downstream targets to control cell migrations (Luo and Raper 1994; Nobes and Hall 1995). Ultimately, signaling regulates actin dynamics that drive cell motility (Lauffenburger and Horwitz 1996; Mitchison and Cramer 1996).

Migratory cells must regulate molecules involved in cell motility, such as cell-surface receptors and signal transduction molecules, to ensure that cells or growth cones migrate at the proper time, in the appropriate direction, and along the correct path. Genetic analysis indicates that some of this regulation occurs transcriptionally. One of the best studied examples of a transcriptional regulator that controls the migration of a cell is the *Caenorhabditis elegans* gene *mab-5*, which encodes a homeoprotein that acts cell autonomously to direct the migrations of the QL neuroblast and its descendants (Chalfie *et al.* 1983; Kenyon 1986; Costa *et al.* 1988; Salser and Kenyon 1992). Normally, QL descendants migrate posteriorly, whereas analogous QR descendants located on the contralateral side of the animal migrate anteriorly (Sulston and Horvitz 1977). Loss of *mab-5* function causes QL to migrate anteriorly like QR, whereas expressing *mab-5* ectopically in the QR descendants causes them to migrate posteriorly (Kenyon 1986; Salser and Kenyon 1992). These results indicate that *mab-5* controls the expression of proteins that direct QL and its descendants posteriorly.

In addition to molecules like MAB-5 that act specifically to regulate a cell's migratory behavior, other tran-

Corresponding author: Wayne Forrester, Department of Molecular and Cell Biology, 401 Barker Hall, University of California, Berkeley, CA 94720-3204. E-mail: forrestr@mendel.berkeley.edu

scriptional regulators act more globally to control additional aspects of a cell's differentiation. The *C. elegans* gene *egl-5*, for example, encodes a homeoprotein that acts cell autonomously to specify HSN fate (Desai *et al.* 1988; Chisholm 1991; Wang *et al.* 1993). Loss of *egl-5* function disrupts not only HSN migration, but later aspects of HSN differentiation, such as neurotransmitter synthesis.

To identify genes required for cell migration and differentiation, we screened for mutants with defects in the migrations of the *C. elegans* canal-associated neurons (CANs). The CANs are a pair of bilaterally symmetric neurons that are born in the head and migrate posteriorly to the middle of the animal during embryogenesis. The CANs extend axons anteriorly and posteriorly along the lateral body wall and express two homeodomain proteins, CEH-10 and CEH-23 (White *et al.* 1986; Wang *et al.* 1993; Svendsen and McGhee 1995). Our screens identified mutations in 14 genes required for CAN cell migration, including the first *ceh-10* mutations. Analysis of *ceh-10* mutants revealed that CEH-10 specifies CAN fate. Reduction of *ceh-10* function results in CANs that partially fail to migrate. Complete loss of *ceh-10* function results in CANs that fail to migrate and do not express CEH-23 or CEH-10.

MATERIALS AND METHODS

Strains and genetics: Strains were grown at 20° and maintained as described (Brenner 1974). In addition to the wild-type strain N2, strains with the following mutations were used in this work.

*LGI: cam-2(gm124), dpy-5(e61), let-204(e1719), syc-3(gm135), unc-11(e47), unc-54(e1092), unc-73(gm33), unc-73(gm67), unc-73(gm123), unc-95(su33*sd*), eDf3.*

LGII: cam-1(gm105), cam-1(gm122), rol-6(e187), unc-4(e120), mnDf16.

*LGIII: ceh-10(gm58), ceh-10(gm71), ceh-10(gm100), ceh-10(gm120), ceh-10(gm127), ceh-10(gm131), ceh-10(gm133), daf-2(e1370), dpy-17 (e164), dpy-18(e364), fam-1(gm85), ina-1(gm144), lin-12(n676*sd *n909), sDf121, syc-1(gm126), syc-2(gm132), unc-32(e189), unc-69 (e587), yDf10.*

*LGIV: bli-6(sc16), dpy-20(e1282*ts*), epi-1(gm57), epi-1(gm121), epi-1(gm139), epi-1(gm146), epi-1(ky152), fam-2(gm94), kyIs5* [*ceh-23-unc-76-gfp::lin-15*], *lin-1(e1275), sDf23, unc-5(e53), unc-24(e128), unc-30(e191).*

LGV: unc-34(gm104), unc-34(gm114), unc-34(gm115), unc-34(gm134), unc-34(e566), vab-8(gm99), vab-8(gm138), vab-8(e1017).

LGX: kyIs4 [*ceh-23-unc-76-gfp::lin-15*], *mig-2(gm38), mig-2-(gm103*sd*), mnDf1.*

dpy-5(e61), dpy-17(e164), dpy-18(e364), unc-4(e120), unc-5(e53), unc-11(e47), unc-24(e128), unc-30(e191), unc-32(e189), unc-34(e566), and *unc-69(e587)* were described by Brenner (1974). *dpy-20(e1282*ts*)* was described by Hosono *et al.* (1982), *bli-6(sc16)* by Park and Horvitz (1986), *epi-1(ky152)* by S. Clark and C. I. Bargmann (personal communication), *let-204(e1719)* by Anderson and Brenner (1984), *lin-12(n676*sd *n909)* by Greenwald *et al.* (1983), *unc-54(e1092)* by Waterston *et al.* (1980), *unc-73(gm33)* by D. Parry, P. Baum and G. Garriga (personal communication), *unc-95(su33*sd*)* by Zengel and Epstein (1980) and *vab-8(e1017)* by Manser and Wood (1990). The chromosomal rearrangement *eDf3* was described by Anderson and Brenner (1984), *mnDf1* by Meneely and Herman (1979), *mnDf16* by Sigurdson *et al.* (1984), *yDf10* by DeLong *et al.* (1993). *sDf23* was isolated by D. Baillie (personal communication), and *sDf121* by H. Stewart, D. Collins and D. Baillie (personal communication). The LGIII balancer *qC1* was described by Austin and Kimble (1989). The *ceh-23-gfp* transgene will be described elsewhere (J. A. Zallen and C. I. Bargmann, unpublished results). Briefly, the GFP coding region was fused to the *ceh-23* 5′ regulatory region and coding sequence up to amino acid 25 of the homeodomain (Wang *et al.* 1993). Amino acids 1–197 of the Unc-76 protein (Bloom and Horvitz 1997) were included to enhance staining of neuronal processes. The *ceh-23-gfp* transgene was injected with the *lin-15* plasmid pJM23 (Huang *et al.* 1994) as a coinjection marker. *kyIs5* is a *ceh-23-gfp* reporter transgene that is integrated on LGIV, and *kyIs4* is the same reporter integrated on LGX (J. A. Zallen and C. I. Bargmann, personal communication). *pInt1*[*ceh-10-lacZ::rol-6*] and *pEx9*[*ceh-10::rol-6*] were described in Svendsen and McGhee (1995).

Because most of the mutants were isolated in a strain containing the *kyIs5* reporter, we removed this transgene from the mutants by crossing to wild type. The *epi-1* alleles *gm121*, *gm139* and *gm146*, and the *fam-2(gm94)* allele are tightly linked to *kyIs5* and have not been separated from the reporter.

Most phenotypes were tabulated from homozygous mutant animals derived from homozygous parents. However, we could not score *ceh-10(gm58), unc-73(gm67), unc-73(gm123)* and *epi-1(gm139)* mutant progeny of homozygous parents. Because *ceh-10(gm58)* homozygotes die as larvae, we examined the phenotypes of homozygous *ceh-10* animals from *ceh-10(gm58)/qC1* hermaphrodites. Because self-progeny of parents homozygous for *unc-73(gm67)* and *unc-73(gm123)* rarely survive to adulthood, we examined phenotypes of homozygous *unc-73* animals from *unc-73* +/+ *dpy-5(e61)* hermaphrodites. Similarly, because *epi-1(gm139)* homozygotes are sterile, we examined phenotypes of homozygous *epi-1(gm139)* animals from + *epi-1(gm139)* + /*dpy-20(e1282*ts*)* + *unc-30(e191)* hermaphrodites.

Screens: Wild-type animals were mutagenized with EMS as described (Brenner 1974). Mutagenized hermaphrodites were cultured individually and allowed to self-fertilize. Three F_1 progeny of each parent were cultured individually, allowed to self-fertilize, and screened for the presence of withered tails (Wit) or clear larvae (Clr) offspring. Lethal or sterile mutants were maintained by selecting heterozygous siblings. Genes were mapped as described in Table 1. Once the genes were mapped, lethal or sterile mutations were balanced by generating animals heterozygous for the mutation and for a chromosome bearing mutations that result in visible phenotypes. CAN cells in candidate Cam mutants were examined by crossing *kyIs4* or *kyIs5* GFP reporter transgenes into the mutant strains and determining CAN cell position by fluorescence microscopy. We examined the progeny of approximately 1000 mutagenized F_1 parents and identified two Wit mutants with CAN migration defects [*epi-1(gm57)* and *unc-73(gm67)*] and two Clr mutants that lacked differentiated CANs [*ceh-10(gm58* and *gm71)*].

In the second screen, animals bearing the *kyIs5* [*ceh-23-unc-76-gfp::lin-15*] transgene were mutagenized and cultivated as described for the first screen (Brenner 1974). From each F_1, approximately 20 first larval stage F_2 progeny were transferred to 5% agar pads on microscope slides. To determine CAN cell position by GFP expression, animals were examined on a Nikon Labophot microscope equipped with epifluorescence. Animals were illuminated using a Nikon BV-2 filter set and a 40× dry objective. F_1s that segregated 25% or more progeny

TABLE 1

CAN migration gene mapping data

Gene	LG[a]	Genotype of heterozygote (F_1)	F_2 phenotype[b]	Number[c]
cam-2	I	*cam-2(gm124)/unc-95(su33sd)*	Unc	0/32
		cam-2(gm124)/let-204(e1719) unc-54(e1092)	Unc	9/9
syc-3	I	*syc-3(gm135)/dpy-5(e61) unc-11(e47)*	Dpy	9/10
			Unc	0/8
cam-1	II	*cam-1(gm122)/rol-6(e187) unc-4(e120)*	Rol	2/15
			Unc	2/4
fam-1	III	*fam-1(gm85)/daf-2(e1370) dpy-17(e164)*	Daf	2/3
ceh-10	III	*ceh-10(gm120)/dpy-17(e164) unc-32(e189)*	Dpy	1/14
			Unc	11/12
syc-1	III	*syc-1(gm126)/dpy-17(e164) unc-32(e189)*	Dpy	2/2
			Unc	0/5
		syc-1(gm126)/unc-69(e587) dpy-18(e364)	Dpy	5/5
			Unc	0/2
epi-1	IV	*epi-1(gm121) kyIs5/unc-5(e53) dpy-20(e1282ts)*	Unc	2/4
			Dpy	1/10
fam-2	IV	*fam-2(gm94)bli-6(sc16)*	Wit	2/18
syc-2	X	*syc-2(gm132)/in-15(n765ts)*	Unc	0/15

Two- and three-factor crosses were performed as described by Brenner (1974). For two-factor crosses, we picked *A* homozygotes from heterozygotes of the genotype *c*/*a*. From heterozygotes of the genotype *c*/*ab*, we picked *A* non-*B* and *B* non-*A* recombinants, and their progeny were examined for the expression of the *C* phenotype. *c* represents the Cam gene mapped with respect to *a* or *b* genetic markers. *C* represents the Cam mutant phenotype and *A* and *B* represent marker phenotypes. Data for a single allele of each gene are presented. For genes represented by additional alleles identified in our screens, map positions were verified using two- or three-factor mapping or deficiency mapping. We only show our mapping data for previously unpublished genes.

[a] Linkage group to which the mutation maps.

[b] The phenotype of the heterozygote progeny picked in both two- and three-factor mapping experiments.

[c] For two-factor crosses, this ratio indicates the number of F_2 progeny that segregate the c mutation out of all F_2 progeny scored. For three-factor crosses, this ratio indicates the number of F_2 progeny that segregate *C* out of all F_2 progeny scored.

with misplaced or missing CANs were characterized further. Lethal or sterile mutants were maintained as described for the first screen.

All mutants were outcrossed to wild type at least three times to remove unlinked mutations. The *kyIs5* GFP reporter was also removed from all strains identified in the GFP screen by mating to wild type and reisolating the mutation in the absence of *kyIs5* (except *gm121*, *gm139*, *gm146* and *gm94*, which are all tightly linked to *kyIs5*). To determine CAN position, the *kyIs5* reporter was crossed into all mutants except *gm57*, which maps near the position of *kyIs5* integration, using standard genetic methods. CAN cell position was determined in *gm57* mutants by crossing in *kyIs4*.

Complementation tests: Mutations that mapped near one another, or near other mutations known to disrupt cell migration, were tested for complementation. This general strategy is illustrated here with *gm121*, a mutation identified in the GFP screen that maps near *epi-1*, a gene required for the migrations of several cells (Forrester and Garriga 1997). Heterozygous *gm121* males were crossed into *epi-1(ky152) unc-24(e128)* (kindly provided by S. Clark and C. Bargmann). Cross-progeny were identified because they no longer displayed the Unc-24 phenotype. Half of these cross-progeny resembled *epi-1* mutants. In addition, these animals had misplaced CAN cells. Thus, based on mapping and complementation, *gm121* is an *epi-1* allele.

We have not been able to eliminate the possibility that *gm135* is an unusual allele of *unc-73*. We have mapped *gm135* and *unc-73* by placing the mutations in *trans* to *unc-11(e47) dpy-5(e61)* and assessing whether recombinants in this interval carry the *syc-3* or *unc-73* mutation. We find that zero of eight Unc non-Dpy and nine of 10 Dpy non-Unc recombinants in this interval carry the *gm135* mutation and one of nine Unc non-Dpy and 19 of 24 Dpy non-Unc carry the *unc-73* mutation. *gm135* animals exhibit a "loopy" Unc phenotype in which animals move with exaggerated body curvature, whereas *unc-73(gm33)* animals rarely move. Although *gm135/unc-73(gm33)* animals are generally not Unc (rare animals are loopy Unc), their CANs are misplaced as often as in *gm135* homozygotes, indicating that *gm135* complements *unc-73* for its movement defects, but not for its CAN migration defects (not shown). *gm135/qDf3* hemizygotes are loopy Unc, similar to *gm135* mutants alone, and have misplaced CANs. *unc-73(gm33)/qDf3* hemizygotes are occasionally loopy Unc and have misplaced CANs. The simplest interpretation of these data is that *gm135* defines a new gene, *syc-3*, which is uncovered by *qDf3*. However, we cannot rule out the alternative model in which *syc-3* is an unusual allele of *unc-73* and that *qDf3* deletes sequences that would complement the CAN cell migration defect of *unc-73* mutants.

Phenotypic characterization: To quantitate phenotypic defects of mutant strains, homozygous viable lines were cultivated at 20°. Individual adult animals were examined for Wit, uncoordinated movement (Unc), egg-laying defective (Egl) and multiple vulvae (Muv) phenotypes, and individual early-stage larvae were examined for Clr or lumpy (Lmp) pheno-

TABLE 2

Behavioral and morphological phenotypes displayed by Cam mutants

Genotype	Percent Clr	Percent Wit	Percent Unc[a]	Percent Egl	Percent Muv	Percent Lmp
Wild type	0 (80)	0 (55)	0 (55)	0 (20)	0 (55)	0 (80)
kyIs5	0 (56)	0 (55)	0 (55)	80 (20)	0 (55)	2 (56)
cam-1(gm105)	0 (77)	9 (55)	87 (53)	70 (20)	0 (53)	6 (77)
cam-1(gm122)	38 (81)	20 (40)	100 (38)	35 (20)	0 (32)	0 (84)
cam-2(gm124)	19 (83)	18 (61)	100 (61)	40 (20)	10 (61)	1 (84)
ceh-10(gm58)[b]	100 (54)	NA	NA	NA	NA	0 (54)
ceh-10(gm120)	3 (72)	23 (70)	15 (68)	10 (20)	19 (53)	0 (72)
ceh-10(gm127)	0 (80)	36 (80)	34 (70)	10 (20)	16 (63)	0 (80)
epi-1(gm57)[c]	0 (79)	12 (49)	100 (49)	0 (20)	22 (49)	47 (79)
epi-1(gm121)	29 (90)	8 (47)	79 (47)	20 (20)	11 (47)	47 (90)
epi-1(gm139)	0 (29)	40 (38)	100 (51)	0 (20)	11 (26)	100 (29)
epi-1(gm146)	2 (56)	8 (66)	64 (75)	0 (20)	3 (38)	71 (56)
fam-1(gm85)	0 (36)	15 (34)	77 (35)	15 (20)	0 (29)	83 (36)
fam-2(gm94)	0 (44)	3 (59)	7 (60)	60 (20)	0 (59)	32 (59)
ina-1(gm144)	0 (47)	18 (33)	83 (36)	30)20)	0 (29)	30 (46)
mig-2(gm38)	0 (85)	0 (46)	100 (46)	35 (20)	2 (46)	3 (85)
mig-2(gm103)	0 (71)	21 (63)	100 (63)	55 (20)	12 (63)	1 (71)
syc-1(gm126)	1 (79)	0 (60)	35 (60)	55 (20)	0 (60)	4 (79)
syc-2(gm132)	0 (56)	0 (44)	100 (44)	0 (20)	0 (44)	0 (56)
syc-3(gm135)	0 (76)	0 (55)	29 (58)	0 (20)	0 (55)	1 (76)
unc-34(gm104)	0 (72)	4 (48)	100 (48)	0 (20)	0 (48)	1 (72)
unc-34(gm114)	0 (59)	0 (53)	100 (53)	0 (20)	0 (58)	5 (59)
unc-34(gm115)	0 (89)	0 (58)	100 (58)	0 (20)	0 (58)	10 (81)
unc-34(gm134)	2 (63)	0 (54)	100 (54)	0 (20)	0 (54)	3 (63)
unc-73(gm67)	0 (39)	18 (50)	100 (50)	85 (20)	10 (50)	0 (39)
unc-73(gm123)	0 (28)	20 (51)	100 (51)	75 (20)	12 (51)	0 (28)
vab-8(gm99)	3 (85)	90 (67)	97 (67)	15 (20)	25 (67)	3 (85)
vab-8(gm138)	3 (77)	85 (72)	96 (72)	10 (20)	28 (72)	0 (77)

Percentage of animals displaying the mutant phenotype is followed in parentheses by the number of animals scored. See materials and methods for a description of how the different phenotypes were scored. Most mutants were characterized in the absence of the *kyIs5* reporter, except for *epi-1(gm121, gm139, gm146)* and *fam-2(gm94)* (see materials and methods). The presence of *kyIs5* enhances the Wit phenotype of Cam mutants and causes an Egl phenotype.

[a] Severity of Unc ranged from animals that moved reasonably well, but with exaggerated sinusoidal body waves (*e.g.*, *syc-3*(*gm135*)), to animals that were immobile (*e.g.*, *mig-2(gm103sd)*).

[b] *ceh-10* strong mutations result in larval lethality and therefore phenotypes exhibited at later stages could not be determined. Although only data for *gm58* is presented, *gm71*, *gm100*, *gm131* and *gm133* behaved similarly to *gm58*.

[c] Because *epi-1* mutants are sterile or partially sterile, the penetrance of the Egl defect is reduced.

types (Table 2). Because the Egl phenotype is transient, we scored Egl by culturing 20 late larval stage animals and monitoring them daily for retention of greater than 15–20 embryos or for hatched larvae within the parent. Wit, Unc and Muv phenotypes were scored by counting adults in random-staged populations that did and did not exhibit the phenotype. Clr and Lmp phenotypes were scored by counting young larvae that did and did not exhibit the phenotype. Phenotypes of mutants not viable as homozygotes were tabulated by monitoring homozygous mutant offspring of heterozygous parents.

Genetic analysis of mutations: To determine whether mutations in newly identified genes were enhanced by deficiencies, we compared the phenotypes of *m*/*Df* to that of *m*/*m*, where *m* is the mutation and *Df* is a deficiency for the locus. To examine *cam-1/Df* animals, we generated a *rol-6(e187) cam-1/mnDf16* strain and examined *rol-6 cam-1/mnDf16* self-progeny for the phenotypes shown in Table 3. *mnDf16* deletes *cam-1*, but not *rol-6*, so non-Rol self-progeny will be hemizygous (*m*/*Df*) for the *cam-1* mutation. Strains were scored in the presence of homozygous *kyIs5* (CAN position column of Table 3) or in its absence (all other columns of Table 3) for behavioral or morphological defects. To examine *fam-2*/*sDf23* animals, we generated *fam-2 kyIs5*/*sDf23* animals by crossing *fam-2 kyIs5* heterozygous males to *sDf23*/+ hermaphrodites. From *fam-2 kyIs5*/*sDf23* animals, *fam-2 kyIs5*/*sDf23* self-progeny were identified by their reduced GFP fluorescence, and their phenotypes were scored. To confirm that the animals scored contained *sDf23*, each animal was transferred to a plate and shown to segregate 1/4 dead embryos. To examine *syc-3*/*Df* animals, we generated *syc-3 dpy-5*/*qDf3* animals. *qDf3* deletes *syc-3*, but not *dpy-5*, so non-Dpy self-progeny are hemizygous for *syc-3*. To examine *syc-2/Df*, we generated *syc-2/mnDf1* and scored the phenotypes. We verified that animals harbored *Df* by culturing each animal individually and determining that it segregated 1/4 dead embryos. The phenotype of *syc-1/Df* was not determined.

cam-2 was not deleted by *eDf3*.*fam-1* was not deleted by *yDf10* or by *sDf121*. Chromosomal deficiencies that delete *ceh-*

TABLE 3

Phenotypes of hemizygous mutant strains

Allele	CAN position[b]	Percent animals that display mutant phenotype[a]					
		Clr[c]	Wit	Unc	Egl	Muv	Lmp[c]
cam-1(gm105)	34 ± 34 (56)	0 (77)	9 (55)	87 (53)	35 (20)	0 (53)	7 (77)
cam-1(gm105)/mnDf16	16 ± 23 (30)	0 (69)	15 (40)	85 (40)	35 (20)	0 (40)	4 (69)
cam-1(gm122)	7 ± 3 (25)	1 (70)	20 (50)	100 (50)	5 (20)	2 (50)	0 (70)
cam-1(gm122)/mnDf16	12 ± 18 (27)	8 (66)	16 (61)	100 (56)	37 (19)	0 (62)	2 (66)
fam-2(gm94)[d]	35 ± 12 (47)	0 (44)	3 (59)	7 (60)	60 (20)	0 (59)	32 (59)
fam-2(gm94)/sDf23	80 ± 22 (26)	0 (50)	15 (13)	93 (13)	8 (13)	0 (13)	0 (50)
syc-2(gm132)	88 ± 19 (53)	0 (56)	0 (44)	100 (44)	0 (20)	0 (44)	0 (56)
syc-2(gm132)/mnDf1	89 ± 15 (22)	0 (65)	0 (31)	100 (31)	0 (31)	0 (31)	0 (65)
syc-3(gm135)	55 ± 31 (38)	0 (76)	0 (55)	29 (58)	0 (20)	0 (55)	1 (76)
syc-3(gm135)/qDf3	77 ± 29 (32)	0 (62)	0 (57)	95 (57)	0 (20)	0 (57)	0 (620

[a] Percentage of animals displaying the mutant phenotype is followed in parentheses by the number of animals scored. See materials and methods for a description of how the different phenotypes were scored.

[b] Average distance CAN cell migrated expressed as a percentage of the distance traveled in wild-type animals (see materials and methods). CAN position in *kyIs5* animals is 98 ± 5%. *kyIs5* provides expression of GFP in the CAN cells.

[c] We were unable to distinguish homozygous mutant first stage larvae from hemizygous mutants. Therefore, these numbers include both.

[d] Two doses of *kyIs5* increases the severity of CAN cell migration defects of Cam mutants and causes an Egl phenotype, whereas one dose of *kyIs5* has no effect. *fam-2* hemizygotes are probably less Cam and Egl than fam-2 homozygotes, because they have only one copy of *kyIs5*.

10 are not currently available. Therefore, we were unable to assess whether the phenotypes of these mutants were enhanced by chromosomal deficiencies.

***ceh-10* rescue:** To determine whether the wild-type *ceh-10* gene could rescue *ceh-10* mutant phenotypes, we generated strains of the genotype *ceh-10(gm58), pEx9*[*ceh-10::rol-6*], and *ceh-10*(*gm127*)*; pEx9*[*ceh-10::rol-6*]. *pEx9* is described in Svendsen and McGhee (1995). Almost all viable offspring from *ceh-10(gm58); pEx9* parents were Rol, indicating that the wild-type *ceh-10* gene present on the extrachromosomal array rescued the lethality of *ceh-10(gm58)*. The CANs were positioned normally in both *ceh-10(gm58); pEx9* and *ceh-10(gm127); pEx9* Rol animals, demonstrating that wild-type *ceh-10* also rescued the CAN cell migration defect.

Sequencing *ceh-10* alleles: To determine the DNA sequence of the coding region and the intron-exon boundaries of mutant *ceh-10* alleles, DNA was cloned by polymerase chain reactions (PCR) from single mutant worms (Williams *et al.* 1992). To amplify the *ceh-10* gene, we used two sets of primers: 5′-dGATGAATTCTCGACTACTGCACACCGG-3′ [127–109; numbers indicate nucleotide position in the genomic sequence beginning at the A of the initiator methionine (Svendsen and McGhee 1995)] and 5′-dGCCATCGATCCCCAG GTTTTCTCGG-3′ (1055–1039) to amplify the 5′ half of the gene, and 5′-dGATGAATTCGGCTTACTTACTGAAACCTGA GACC-3′ (913–933) and 5′-dGCCATCGATTGTTTCCTGACC GCTC-3′ (2064–2049) to amplify the 3′ half. The first primer for each reaction contained an *Eco*RI site, and the second primer contained a *Cla*I site. We cleaved the PCR products with *Eco*RI and *Cla*I and purified them by electrophoresis in 0.8% low melting temperature agarose (Sambrook *et al.* 1989). We cloned the products into *Cla*I and *Eco*RI cleaved pBSKS+ (Stratagene). DNA was extracted from the transformed cells and sequenced using the following primers: 5′-dGATGAATTCTCGACTACTGCACACCGG-3′ (1054–1072), 5′-dCACGGATATTGTCCTCAG-3′ (168–185), 5′-dCCAATCT CAACATCAGCGG-3′ (359–377), 5′-dGATGAATTCGGCTTA CTTACTGAAACCTGAGACC-3′ (913–933), 5′-dAATTACCCT GAACCACC-3′ (1602–1618). We determined the DNA sequence of the mutant *ceh-10* genes from three independent PCR reactions.

Identification of AIY in *ceh-10* mutants: To determine whether AIY cells were produced but failed to express *ceh-10-lacZ* or *ceh-23-gfp* transgenes in strong *ceh-10* mutants, or were absent, we examined *ceh-10(gm58)* mutants for the presence of AIY cells by Nomarski microscopy. AIY was identified by its characteristic location in these animals. AIY cells were detected in 15 of 16 sides of animals examined.

Histochemical and immunocytochemical staining: We detected β-galactosidase activity histochemically in wild-type and *ceh-10(gm58)* first stage larvae (L1) that carried the *pInt1*[*ceh-10-lacZ::rol-6*] transgene. We transferred several worms in 200 μl water to a multiwell glass dish. The glass dish was placed under vacuum until the water had evaporated. Three hundred microliters of −20° acetone was added to worms and then allowed to evaporate. One hundred to two hundred microliters of staining solution (300 μl 2× phosphate buffer [360 mM Na_2HPO_4, 40 mM NaH_2PO_4, 10 μl 1 M $MgCl_2$], 100 μl 100 mM Redox buffer [50 mM K ferricyanide, 50 mM K ferrocyanide], 4 μl 1% SDS, 400 μl dH_2O, 12 μl 2% X-gal in dimethyl formamide) was added to worms and allowed to incubate at room temperature for 1 hr to overnight in a sealed, humidified container (Fire *et al.* 1990). Animals were stained with antibodies to the neurotransmitter GABA as described previously (Wightman *et al.* 1996).

RESULTS

Screens for cell migration mutants: To identify mutants defective in CAN development and migration, we performed two mutant screens. In the first screen, we took advantage of the Clr and Wit visible phenotypes that are displayed by animals lacking normal CAN function. Killing both CANs in newly hatched larvae causes ani-

mals to die with a distinctive transparent appearance, the clear (Clr) phenotype (Figure 1B; Forrester and Garriga 1997). In addition, mutants with misplaced CAN cell bodies often develop a dramatic withering of the posterior half of the animal, the withered-tail (Wit) phenotype (Figure 1E; Manser and Wood 1990; Wightman *et al.* 1996; Forrester and Garriga 1997). We screened the progeny of individual F_1s from mutagenized parents for the Clr or Wit phenotypes and then determined whether these mutants displayed CAN defects. By screening the progeny of approximately 1000 F_1 animals, we identified two Wit mutants with CAN migration defects, *epi-1(gm57)* and *unc-73(gm67)*, and two Clr mutants that lacked differentiated CANs, *ceh-10(gm58* and *gm71)* (Table 2). We also identified eight Clr mutants that had morphologically normal CANs. These mutants were not analyzed further.

In the second screen, we took advantage of a reporter that fused regulatory sequences of *ceh-23*, a *C. elegans* homeobox gene, to *Aequorea victorea* green fluorescent protein (GFP; Chalfie *et al.* 1994). Transgenic animals that contain the *ceh-23-gfp* reporter express GFP in the CANs, as well as several neurons of the head and tail (Figure 2A). We screened the progeny of individual F_1s from mutagenized parents for animals with missing or misplaced CANs by fluorescence microscopy (for examples, see Figure 2, B and C). By screening the progeny of 2567 F_1 animals, we identified 30 mutants. Of these mutants, six were weak or genetically complex and were not pursued. Of the remaining mutants, three lacked differentiated CANs, and 21 had misplaced CANs. Two mutants, *fam-1(gm85)* and *mig-2(gm38)*, were identified in a similar screen for cell migration mutants using Nomarski optics microscopy (D. Parry, P. Baum and G. Garriga, personal communication). Their characterization is included here.

To define the genes identified in the screens, the chromosomal positions of the mutations were mapped using standard two- and three-factor mapping and deficiency mapping (materials and methods, Table 1). Mutations that mapped near one another, or near previously identified genes known to affect cell migrations, were tested for complementation. In this way, the 30 mutations identified in the screens were assigned to 14 genes (Figure 3; Table 1). We identified mutations in the six previously defined genes: *epi-1* (epithelialization defective), *ina-1* (integrin α-subunit), *mig-2* (migration defective), *unc-34*, *unc-73* (uncoordinated movement), and *vab-8* (variable abnormal), and in the seven new genes: *cam-1*, *cam-2* (CAN abnormal migration); *fam-1*, *fam-2* (fasciculation and cell migration defective); and *syc-1*, *syc-2*, and *syc-3* (synthetic Cam). In addition, the first mutations in *ceh-10* were identified. *ceh-10* previously had been identified molecularly as a *C elegans* homeobox-containing gene (Hawkins and McGhee 1990; Svendsen and McGhee 1995).

All three Syc mutants require the presence of *kyIs5*, which contains the *ceh-23-gfp* transgene, to express a penetrant Cam phenotype (Figure 4). *kyIs5* confers a subtle Cam phenotype and enhances the severity and penetrance of the Cam defect in the other mutants. The Syc mutants differ from other Cam mutants, however, in that they require *kyIs5* to express a Cam defect. The *kyIs5* transgene contains a *ceh-10-unc-76-gfp* fusion gene, as well as the gene *lin-15*. The UNC-76 sequences were inserted to help localize GFP to neuronal axons, and the gene *lin-15* was a marker used originally to follow the presence of the transgene. We have not rigorously tested whether *ceh-23*, *unc-76*, *gfp* or *lin-15* sequences, or the site of *kyIs5* integration, confer the Syc phenotype to these mutants.

Phenotypic characterization of Cam mutants: We investigated whether the mutants were Clr or Wit, phenotypes associated with defects in CAN function (Figure 1, B and E; Table 2). We also examined the mutants for uncoordinated movement (Unc), multiple vulvae (Muv), egg-laying defective (Egl), or lumpy larvae (Lmp) phenotypes (Figure 1, C, F and G; Table 2). Finally, we determined whether mutant phenotypes were enhanced when the mutations were placed over a deficiency for the locus (Table 3).

cam-1(gm105, gm122) II: cam-1 mutant animals are Wit, Unc and Egl. The *cam-1* Unc phenotype is distinctive; mutant animals move forward with an exaggerated waveform, often coiling into a tight spiral. In response to high temperatures, high population densities, and limited food, wild-type animals enter a morphologically distinct alternate third larval stage called dauer (Cassada and Russell 1975; Golden and Riddle 1984). In the presence of low population densities and sufficient food, both *cam-1* mutations cause a dauer constitutive phenotype, with approximately 15% of the larvae becoming dauers at 20°. Under these conditions, wild-type animals never become dauers (Cassada and Russell 1975; Golden and Riddle 1984).

The *gm122* allele appears stronger than the *gm105* allele. For example, 9% of *gm105* animals are Wit and 87% are Unc, while 20% of *gm122* animals are Wit and 100% are Unc (Table 2). *gm122* animals are also smaller and grow more slowly than *gm105* animals. Gene dosage experiments suggest that *gm105* reduces *cam-1* function, whereas *gm122* may eliminate it. *cam-1(gm122)/mnDf16* hemizygous animals display most phenotypes with similar frequency and severity to *cam-1(gm122)* homozygotes, whereas *cam-1(gm105)/mnDf16* hemizygous animals are more often Wit and exhibit more severe CAN migration defects than *cam-1(gm105)* homozygotes (Table 3).

cam-2 (gm124) I: cam-2 mutants often die as Clr larvae. Animals that survive to adulthood are often Wit, Unc and Egl. In addition, nearly 10% of the adult animals are multivulval (Muv; Figure 1G). Mutants displaying a severe Wit phenotype are Muv, with ectopic vulvae always located posterior to the vulva (Wightman *et al.*

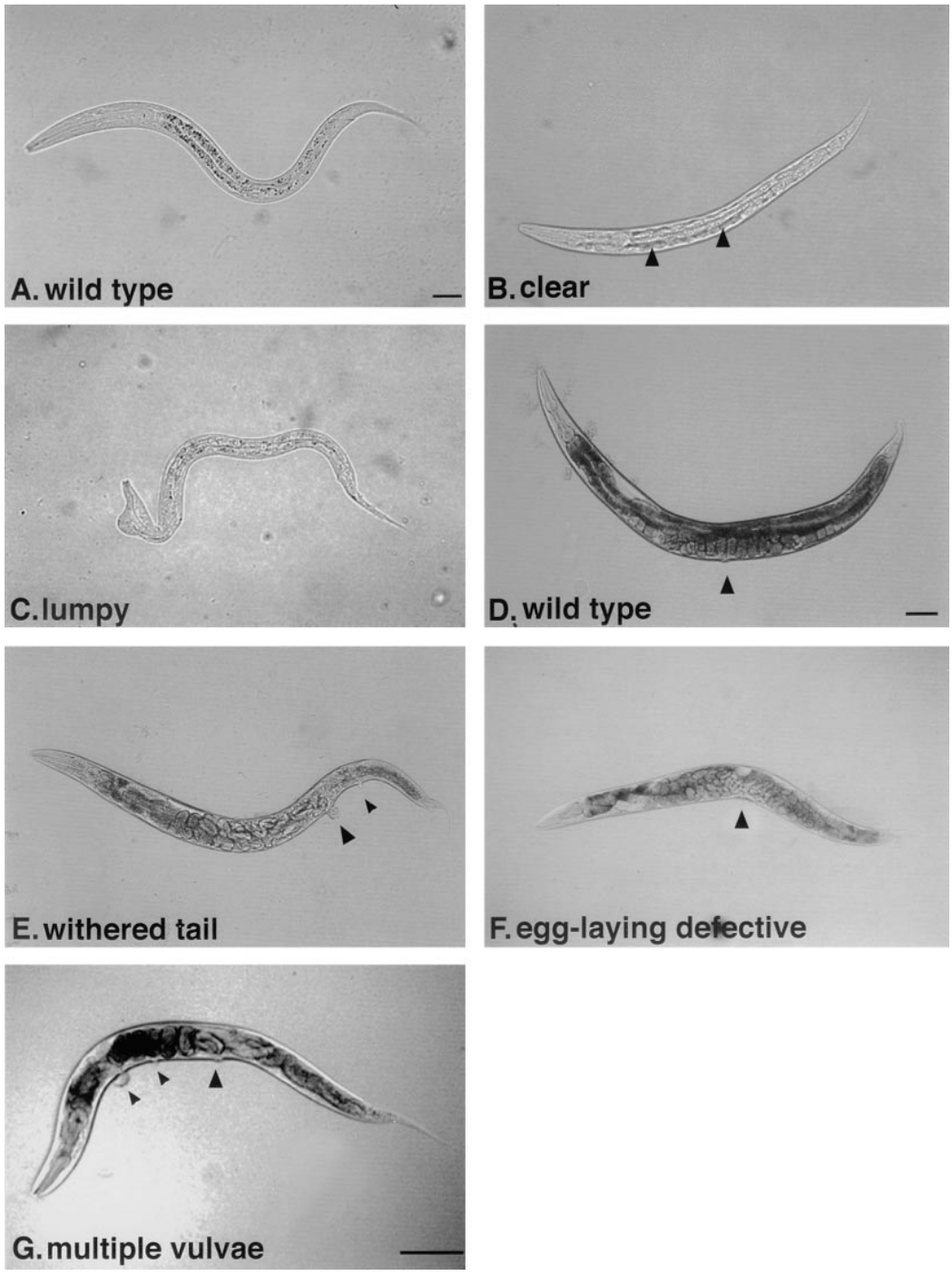

Figure 1.—Cam mutant phenotypes. Lateral views of late first stage larval (A–C) or adult (D–G) hermaphrodites viewed by bright field microscopy. In all panels, anterior is to the left and dorsal is up. (A) Wild-type first stage larva. (B) A *ceh-10(gm58)* first-stage larva that displays the Clr phenotype. Accumulation of fluid between intestine and body wall makes the animals appear translucent or clear (arrowheads). (C) A *fam-1* first stage larva that displays the Lmp phenotype. Note the large ventral protrusion on the head of this animal. (D) Wild-type adult hermaphrodite. Arrowhead indicates the position of the vulva. (E) An adult *vab-8(gm99)* hermaphrodite that displays the Wit phenotype. Note the reduced girth in the region posterior to the vulva (large arrowhead) relative to the anterior half. Wit animals often have protruding vulvae (large arrowhead) and produce ectopic ventral protrusions consisting of vulval cells (small arrowhead). (F) An adult *cam-1(gm105)* hermaphrodite that displays the Egl phenotype. The mutant hermaphrodite has retained additional late-stage embryos (small light ovals visible within the animal). Arrowhead indicates the position of the vulva. (G) An adult *cam-2* hermaphrodite that displays ectopic vulval protrusions (small arrowheads) anterior to the vulva (large arrowhead). Also note that the magnification of this panel is twice that of D–F, reflecting the small phenotype of *cam-2* mutants. Scale bar for A–C shown in A represents 20 μm, and for D=nF, shown in D represents 50 μm. The scale bar in G represents 50 μm.

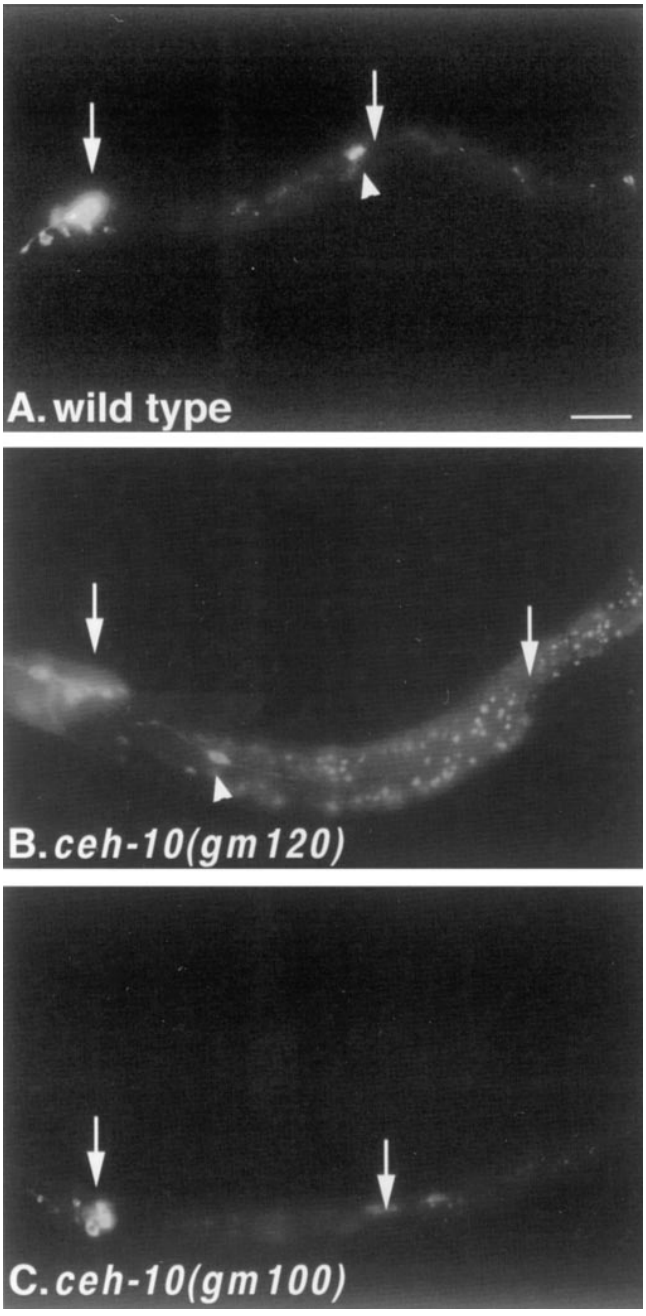

Figure 2.—*ceh-10* mutants are defective in CAN development. Immunofluorescence photomicrographs of wild-type and *ceh-10* mutant larvae bearing the *kyIs5* transgene. All panels show a left lateral view with anterior to the left and dorsal up. The arrowhead indicates the position of the CAN cell body. Left and right arrows indicate positions of the *ceh-23-gfp*-expressing cells in the head and of the gonad primordium in the midbody, respectively. (A) Wild-type early larval stage hermaphrodite. Left CAN is in the middle of animal. (B) *ceh-10(gm120)* early larval stage hermaphrodite. Left CAN is misplaced anteriorly. (C) *ceh-10(gm100)* early larval stage hermaphrodite. The CANs are not detected by *ceh-23-gfp* expression. Small spots seen in each animal are due to intestinal autofluorescence. Scale bar, 20 μm.

1996). By contrast, *cam-2* mutants also develop ectopic vulvae at positions anterior to the vulva, suggesting that the *cam-2* Muv phenotype is not a secondary consequence of tail withering. *cam-2* mutants are often substantially smaller than wild type and exhibit greatly reduced brood sizes (Figure 1G).

fam-1 (gm85) III: fam-1 mutant larvae are often lumpy in appearance and frequently develop notched heads resembling those seen in *vab-3* or *ina-1* mutants (Figure 1F; Chisholm and Horvitz 1995; Baum and Garriga 1997). *fam-1* mutants are often Unc, and occasionally Wit and Egl. In addition, *fam-1* mutants are slightly shorter and fatter than wild type, a phenotype referred to as dumpy (Dpy).

fam-2 (gm94) IV: fam-2 mutants are rarely Wit or Unc (Table 2). Because *fam-2* was identified in the GFP screen and is tightly linked to the GFP reporter, we have been unable to separate it from the reporter. Because hermaphrodites carrying the *ceh-23-gfp* transgene are Egl, we have not established whether *fam-2* hermaphrodites are Egl in the absence of the GFP reporter. *fam-2/sDf23* hemizygous animals are more often Wit and Unc than *fam-2* homozygotes (Table 3). The penetrance of the Egl defect decreases in hemizygous animals. The lower Egl penetrance may be caused by the decreased dose of the *ceh-23-gfp* transgene since this transgene causes the Egl phenotype when homozygous, but not when heterozygous.

syc-1(gm126) III: syc-1 mutants are Dpy, Unc and Egl. The Dpy phenotype is maternally rescued; homozygous *syc-1* self-progeny from a heterozygous hermaphrodite are less Dpy than *syc-1* self-progeny from a homozygous hermaphrodite (data not shown). Similarly, the Cam phenotype of *syc-1* mutants is maternally rescued.

syc-2(gm132) X: syc-2 mutants are Unc, generally exhibiting a strong "kinker" locomotion phenotype. Instead of moving in a smooth sinusoidal wave, *syc-2* mutants kink with moving. *syc-2/mnDf1* animals display the Unc phenotype with similar severity and penetrance to *syc-2* mutants alone (Table 3).

syc-3(gm135) I: syc-3 mutants are weakly Unc, generally exhibiting exaggerated curvature of the body when moving, particularly when moving backward. *syc-3/qDf3* hemizygous animals are more severely Unc, suggesting that *syc-3(gm135)* may reduce, but not eliminate gene function (Table 3).

epi-1 (gm57, gm121, gm139, gm146) IV: epi-1 mutants are Wit, Unc, Muv and Lmp (Table 2). Based on the penetrance of these phenotypes, as well as brood size and viability of the mutant strains, the *epi-1* alleles can be ordered into an allelic series where *gm121* is the weakest, *gm57* and *gm146* are intermediate, and *gm139* is strongest. In addition to the phenotypes described above, *epi-1* mutants are somewhat Dpy and exhibit defects in gonadal morphology (not shown and K. Joh, D. Hall, J. Yochum, I. Greenwald and E. Hedgecock, personal communication). *gm57* and *gm146* have

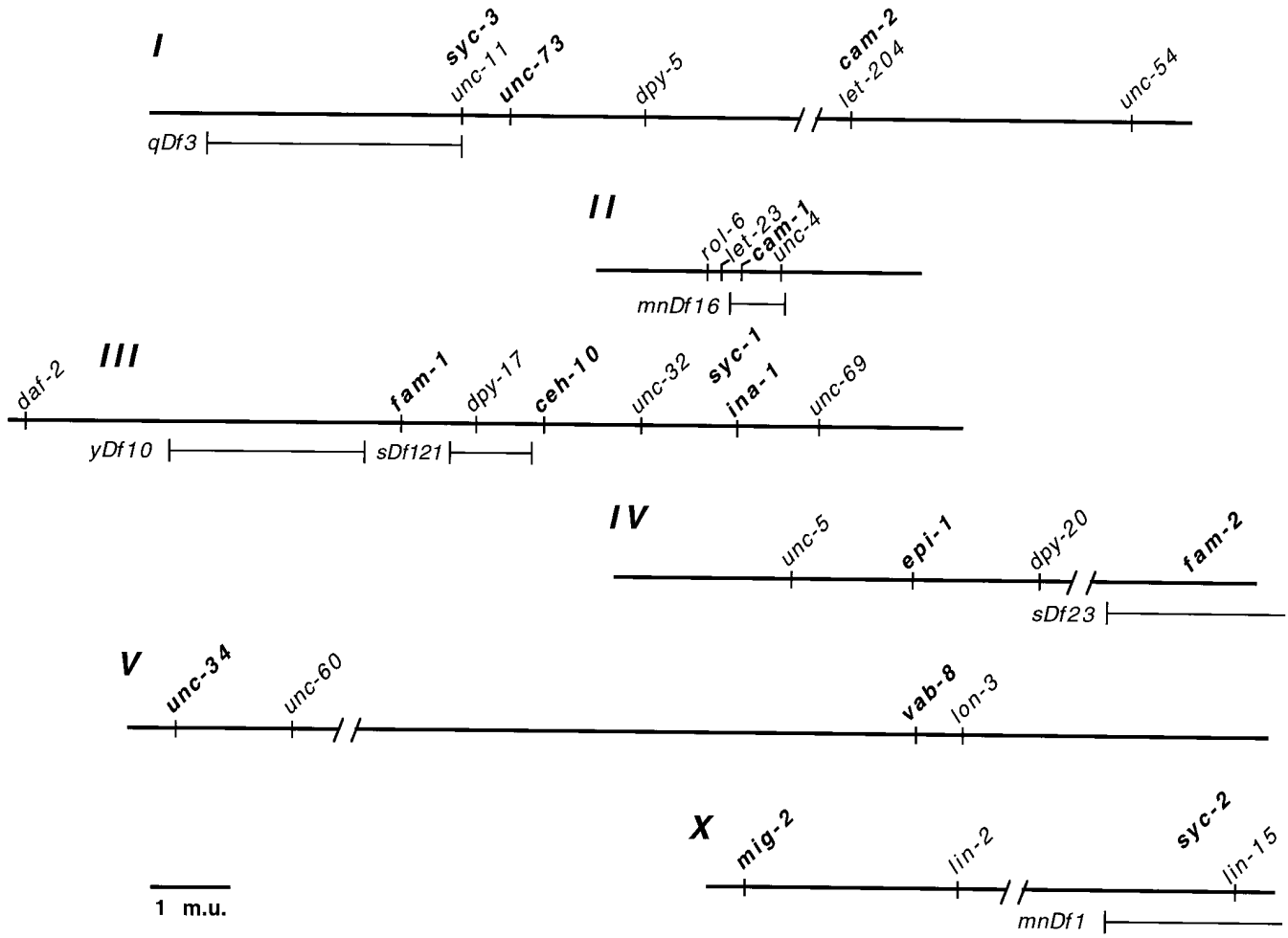

Figure 3.—Map positions of Cam genes. Lines represent the portions of the six *C. elegans* linkage groups where the Cam genes map. Cam genes identified in our screen are in bold print. The other genes represented on the map were used in Cam gene mapping. Cam genes set off from the line have not been mapped precisely relative to indicated markers. The lines below the LGs represent the extents of deficiencies used for mapping. The map positions of the Cam genes is based on previously published results and data presented in Tables 1 and 3.

greatly reduced brood sizes relative to wild type, and *gm139* mutants are sterile. Unlike the other *epi-1* alleles, *epi-1(gm121)* mutants often die as Clr larvae. Because other *epi-1* mutants are not Clr, including the three stronger alleles isolated in our screens, the Clr phenotype of *epi-1(gm121)* mutants may be caused by a second, linked mutation.

ina-1 (gm144) III: ina-1 mutants are Unc, Egl and Lmp, and occasionally Wit. The Unc animals are generally able to move well, but occasionally fail to move smoothly and instead "coil" transiently. *ina-1(gm144)* is likely to represent a partial loss-of-function mutation because stronger mutations in *ina-1* result in larval lethality (Baum and Garriga 1997).

*mig-2 (gm38, gm103*sd*) X: mig-2* mutants are Unc and Egl (Table 2). *mig-2(gm38)* animals are often able to move, but do so poorly, and often exhibit a kinked appearance. Homozygous *mig-2(gm103*sd*)* mutants are severely Unc, as well as Wit and Egl. The mutant animals are generally paralyzed, with a strongly kinked appearance. In addition, *mig-2(gm103*sd*)*, but not *mig-2(gm38)*, mutants often have ectopic laterally positioned vulvae as seen in *unc-40* mutants (Hedgecock *et al.* 1990). *mig-2(gm103*sd*)* is the only obvious semidominant mutation identified in our screens. Although heterozygous animals are rarely Unc, their CANs migrate only an average of 73 ± 22% of their normal distance. By contrast, the CANs of *mig-2(gm38)*/+ heterozygous animals appear normal.

unc-34 (gm104, gm114, gm115, gm134) V: unc-34 mutants exhibit a severe and 100% penetrant Unc phenotype. The animals either fail to move, or do not move with the smooth motion of wild-type animals.

unc-73 (gm67, gm123) I: unc-73 mutants are often Unc, Egl and Wit. In addition, they have ectopic laterally positioned vulvae like those seen in *mig-2(gm103*sd*)* mutants. Some Unc-73 phenotypes are partially maternally rescued. Homozygous self-progeny from heterozy-

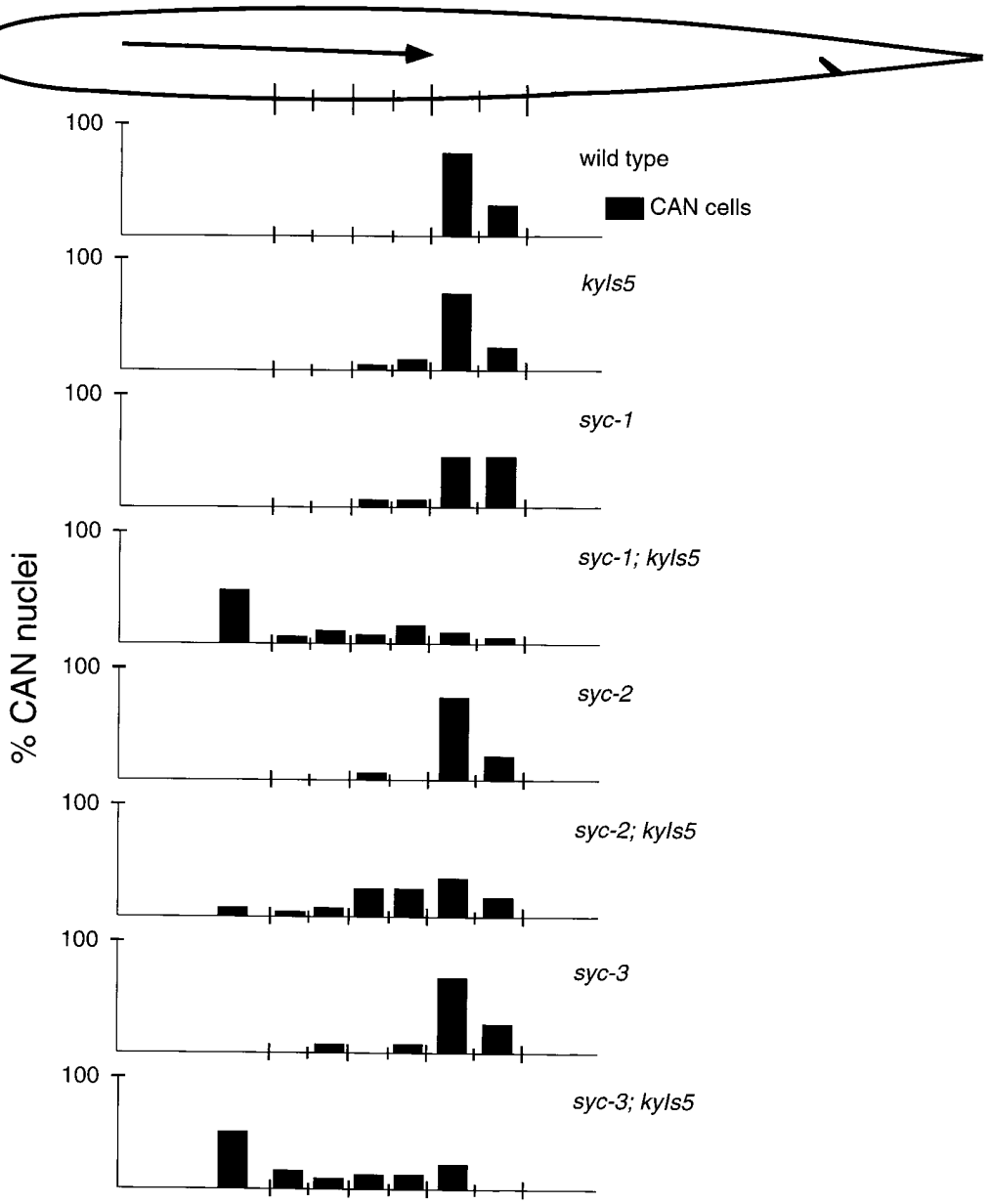

Figure 4.—Cam phenotypes in the Syc mutants. At the top is a schematic representation of a first larval stage (L_1) animal. Anterior is to the left and ventral is down. The arrow indicates the direction and extent of CAN migration. Each vertical line along the ventral side of the worm indicates the positions of hypodermal cell nuclei. The CAN nuclei were scored in newly hatched L_1 animals relative to the indicated hypodermal nuclei. The CAN positions for each strain are represented as a percentage of all the CANs scored in the bar graphs below.

gous hermaphrodites are less Wit, do not exhibit lateral vulvae as often, and have larger numbers of progeny than homozygous self-progeny from homozygous hermaphrodites.

vab-8 (gm99, gm138) V: vab-8 mutants are often Wit, Unc, Muv and occasionally Egl. Ectopic vulvae are always located posterior to the vulva (Figure 1E; Wightman *et al.* 1996).

ceh-10 (gm58, gm71, gm100, gm120, gm127, gm131, gm133) III: We isolated seven *ceh-10* mutants of two phenotypic classes. One mutant class, represented by the two alleles *gm120* and *gm127*, are viable. These mutants are occasionally Wit, Unc, Egl and Muv (Table 2). As with *vab-8* mutants, we propose that the Unc and Muv phenotypes of these *ceh-10* mutants result from tail withering (Wightman *et al.* 1996). The CANs of these mutants are partially disrupted in their migrations (Figure 2; Forrester and Garriga 1997). The level of CEH-23-GFP expression appears similar to wild type (Figure 2B). A second mutant class, represented by the five alleles *gm58*, *gm71*, *gm100*, *gm131* and *gm133*, die as Clr larvae. The CANs of these mutants appear com-

pletely disrupted in their migrations (Forrester and Garriga 1997), and they fail to express the *ceh-23-gfp* transgene (Figure 3). The visible and CAN phenotypes of the mutants indicate that *gm120* and *gm127* are weaker than the other *ceh-10* alleles, and thus are partial loss-of-function mutations.

All seven *ceh-10* mutations mapped genetically to a region of LG III that contained *ceh-10*, a gene encoding a homeoprotein that is expressed in the CANs (Svendsen and McGhee 1995). To determine whether our mutations were *ceh-10* alleles, we introduced a wild-type *ceh-10* transgene into *gm58* and *gm127* mutant strains and found that the *gm58* and *gm127* mutant phenotypes were rescued by the *ceh-10* transgene. When carrying the transgene, *gm58* mutants survived to adulthood, and *gm127* adult hermaphrodites were no longer Wit, Unc, Egl or Muv. Furthermore, the CANs of *gm58* mutants expressed the *ceh-23-gfp* transgene and the CANs of both *gm58* and *gm127* mutants were positioned normally.

***ceh-10* mutations:** To determine the molecular nature of the *ceh-10* mutations, we cloned and sequenced *ceh-10* from the mutant strains. The two independent partial loss-of-function mutations, *gm120* and *gm127*, were identical; the conserved GT of the first intron's 5′ splice site was mutated to AT (Figure 5). Presumably splicing still occurs at this site, or from a cryptic site, to produce functional product since these mutations do not eliminate *ceh-10* function. Two of the stronger alleles, *gm58* and *gm71*, were missense mutations, and two, *gm100* and *gm133*, were nonsense mutations (Figure 5). The *gm133* mutation should terminate translation of the protein 10 amino acids into the homeodomain to produce a truncated product that is predicted to lack DNA binding activity. Thus, the strong *ceh-10* alleles are likely to eliminate gene function.

***ceh-10* regulates *ceh-23* and *ceh-10* expression:** Although the partial loss-of-function *ceh-10* mutations disrupt only CAN migration, the more severe mutations also appear to perturb CAN differentiation. By Nomarski optics, CANs are not detected in their proper positions or along their migratory routes (Forrester and Garriga 1997). A complete failure of CAN migration would place the cells among other neurons of the head ganglia, making it impossible to distinguish ectopic CANs from neighboring cells by Nomarski optics. In addition, the CANs fail to express the *ceh-23-gfp* transgene (Figure 2C). The absence of detectable CANs raises several possibilities. The *ceh-10* mutations could disrupt divisions in the CAN lineage in such a way that the CANs are never produced. Alternatively, the CANs could be generated, but then fail to differentiate or die.

In *ceh-10* mutants, the RMED and AIY neurons, which normally express *ceh-10* (Svendsen and McGhee 1995), fail to express differentiation markers. The four RME neurons express the neurotransmitter GABA. RMED, the only RME that expresses *ceh-10*, failed to express detectable levels of GABA in *ceh-10(gm127)* mutants; RMED was not detected by GABA staining in 15/16 mutant animals, whereas it was detected in 14/14 wild-type animals. Like misplaced CANs, the RMED neuron occupies a position that made its identification by Nomarski optics difficult. AIY, an interneuron that expresses both *ceh-10* and *ceh-23* also fails to express *ceh-23-gfp* in strong *ceh-10* mutants (not shown). Unlike the CANs and RMED, the AIY neuron is relatively isolated with three other neurons at the posterior end of the ventral ganglia, making its identification by Nomarski optics straightforward. We have detected AIY in strong *ceh-10* mutants by Nomarski optics, indicating that AIY is produced, but fails to differentiate (materials and methods). We propose that the CANs and RMED are also produced in *ceh-10* mutants, but fail to differentiate.

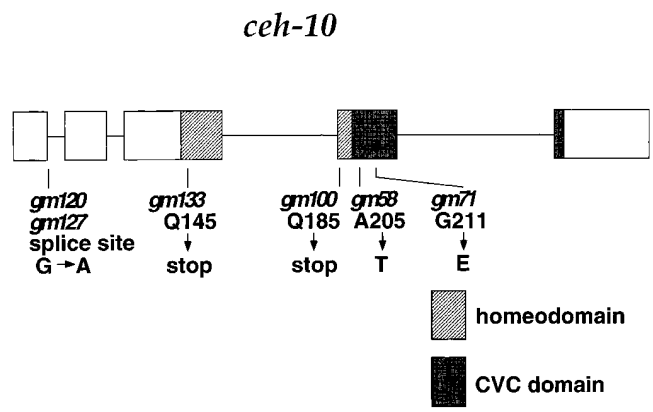

Figure 5.—*ceh-10* mutations. A portion of the *ceh-10* gene is shown beginning at the start codon and ending at the stop codon. Boxes represent coding sequences, and lines represent introns. Positions of the mutations, and the molecular lesions, are indicated.

To determine whether *ceh-10* expression requires *ceh-10* function, we introduced a *ceh-10-lacZ* transgene into a *ceh-10(gm58)* mutant background. In wild type, the *ceh-10-lacZ* transgene is expressed in AIYL/R, CEPDL/R, RID, ALA, RMED, AINL/R, AVJL/R and CANL/R (Figure 6; Svendsen and McGhee 1995). In *ceh-10(gm58)* mutants, we detect no *ceh-10-lacZ* transgene expression (Figure 6). This result suggests that *ceh-10* regulates its own expression.

DISCUSSION

Genetic screens for Cam genes: We used two genetic screens for CAN migration mutants. First, we isolated mutants that were Wit or Clr, phenotypes associated with defects in CAN function. Second, we screened directly for mutants with misplaced or missing CANs in a strain that expressed GFP in the CANs. Although more labor intensive, the second screen proved more productive; screening approximately two and a half times the number of mutagenized chromosomes identified six times as many mutants.

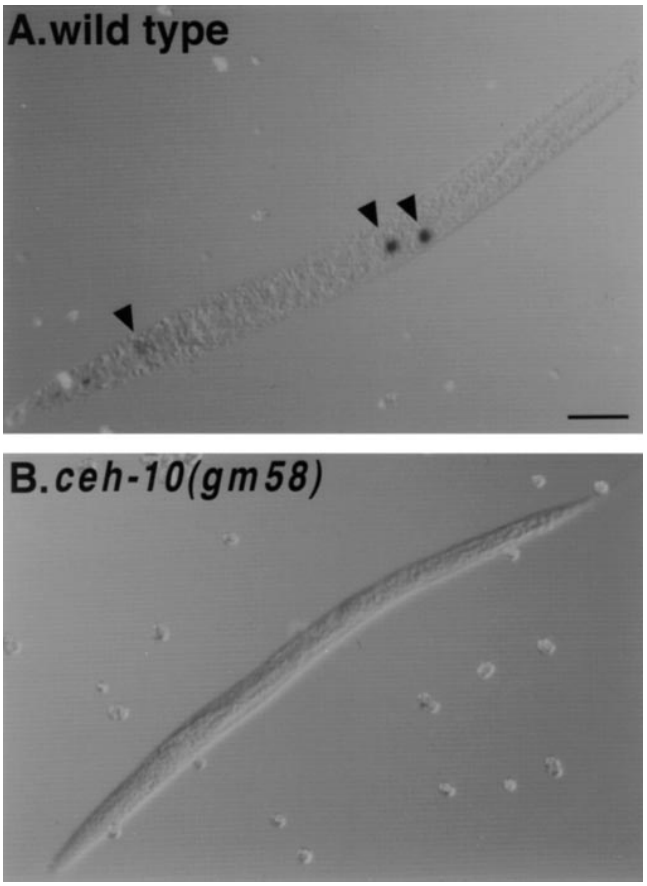

Figure 6.—*ceh-10* expression requires CEH-10 function. Histochemical staining was used to detect β-galactosidase expression from *ceh-10-lacZ* transgene. Anterior is to the left, and dorsal is up. (A) Wild-type transgenic animal expressing β-galactosidase in the CANs and at least one cell in the head (arrowheads). The number of β-galactosidase expressing cells in transgenic animals varies. (B) *ceh-10(gm58)* transgenic animals never express β-galactosidase. Scale bar, 20 μm.

There are two likely explanations for the greater success of the GFP screen. First, nearly half of the mutants isolated in the direct screen were less than 10% Wit or Clr and would have been missed in the Wit and Clr screen. Second, several of the mutants developed slowly. The Wit phenotype is most easily scored in adult animals, while defects visualized by GFP could be scored in younger animals. In the Wit and Clr screen, mutants that are slow to reach adulthood might be lost among the next generation of nonmutant animals.

Three Syc mutants require the presence of *kyIs5* to express the Cam phenotype: mutations in the *syc* genes result in defects in CAN cell migration only when *kyIs5* is present (Figure 4). Mutations in each of the Syc genes results in weak (*syc-1* and *syc-3*) or strong (*syc-2*) Unc phenotypes in the absence of the transgene, suggesting that the mutations disrupt the development or function of additional neurons. The effects on CAN migration are enhanced when the *syc-3* mutation is placed *in trans* to a deficiency, raising the possibility that stronger alleles of this gene would result in CAN migration defects in the absence of *kyIs5*.

Most mutations reduce or eliminate gene function: Our interpretation of the roles played by these genes in CAN cell migration and differentiation assumes that our mutations reduce or eliminate rather than alter gene function. Several considerations support this hypothesis. First, all mutations except *mig-2(gm103*sd*)* result in recessive phenotypes, which are likely to result from reducing or eliminating rather than altering gene function (Park and Horvitz 1986). Second, several of the genes were identified by multiple alleles. We identified seven alleles of *ceh-10*, four alleles each of *epi-1* and *unc-34*, and two alleles each of *cam-1*, *unc-73*, and *vab-8*. Mutations that reduce or eliminate gene function are more common than mutations that alter function (Brenner 1974). Third, we analyzed mutations of *cam-1*, *fam-2*, *syc-2* and *syc-3* in *trans* to chromosomal deficiencies of these loci. For the *cam-1(gm122)* and *syc-2(gm132)* mutations, the phenotypes of hemizygous and homozygous mutants were similar, suggesting that these mutations severely reduce, and possibly eliminate, gene function. For the *cam-1(gm105)*, *fam-2(gm94)* and *syc-3(gm135)* mutations, the phenotypes of hemizygous animals were more severe than those of homozygotes, suggesting that these mutations reduce gene function. Finally, two of the strong *ceh-10* alleles are nonsense mutations in the homeodomain, which should result in truncated proteins that lack DNA binding activity.

The *mig-2(gm103*sd*)* mutation, by contrast, is semidominant. Heterozygous *mig-2(gm103*sd*)*/+ animals are occasionally Unc and have misplaced CANs (not shown), and homozygous *mig-2(gm103*sd*)* animals are more severely Unc and have CANs that are more severely misplaced (Table 2; Forrester and Garriga 1997). The *mig-2(gm38)* mutation, by contrast, appears recessive. These results suggest that *gm103* alters *mig-2* function.

Neural function in the Cam mutants: Two observations suggest that the Clr lethal and Wit phenotypes are related, resulting from defects in CAN function. First, Clr and Wit phenotypes both result from defects in CAN function. Animals lacking CANs, generated by laser microsurgery or by mutation, die as Clr larvae, and Cam mutants are often Wit (Manser and Wood 1990; Wightman *et al.* 1996; Forrester and Garriga 1997). Second, the tails of Wit mutants appear Clr, suggesting that tail withering results from a lack of CAN function in the posterior body. A correlation between defects in outgrowth of the posterior CAN axon and the Wit phenotype further support this hypothesis (Forrester and Garriga 1997).

Cell migration and axon outgrowth defects appear to result in other behavioral and morphological defects. During embryogenesis, the bilaterally symmetric HSNs migrate anteriorly (Sulston *et al.* 1983). Later during larval development, each HSN extends an axon

that innervates the egg-laying muscles to establish synapses that are essential for egg laying (White *et al.* 1986; Desai *et al.* 1988; Garriga *et al.* 1993). *cam-1, cam-2, fam-2, ina-1, mig-2, syc-1* and *unc-73* mutants display significant defects in egg laying. The HSN migration or axon pathfinding defects of *cam-1, fam-2, ina-1, mig-2* and *unc-73* may contribute to the egg-laying defective (Egl) phenotype of these mutants (Forrester and Garriga 1997). Because the HSNs of *cam-2* and *syc-1* mutants appear normal, the Egl phenotype of these mutants results from defects in HSN function or from defects in the development or function of other components of the egg-laying system. Consistent with this view, *cam-2* mutants are abnormal for development of the vulva, the opening though which eggs are laid.

Locomotion in *C. elegans* requires the coordinated contractions of body wall muscles that the nervous system regulates. *cam-1*, *cam-2*, *epi-1*, *fam-1*, *ina-1*, *mig-2*, *syc-2*, *unc-34*, *unc-73* and *vab-8* mutants are usually uncoordinated (Unc). *epi-1*, *fam-1*, *mig-2*, *unc-34* and *unc-73* displayed defects in the morphology of the VD and DD motor neurons, which regulate locomotion (Forrester and Garriga 1997), and *vab-8* mutants displayed defects in the morphology of the interneurons involved in movement (Wightman *et al.* 1996), making it likely that these axon outgrowth defects contribute to Unc phenotypes of these mutants. Possibly, defects in the outgrowth of other axons involved in movement contribute to the Unc phenotype of *cam-1*, *cam-2*, *ina-1* and *syc-2* mutants.

***ceh-10* is a member of a gene family necessary for cell differentiation:** CEH-10 is homologous to Chx10 in mouse and Vsx-1 in goldfish, two proteins that are expressed during retinal development (Levine *et al.* 1994; Liu *et al.* 1994). The proteins are members of the Pax-like class of homeoproteins, containing a conserved octapeptide sequence and Pax-like homeodomain, but lacking the paired-box of Pax homeoproteins. In addition, all three proteins contain a highly conserved 60-amino acid region located immediately C-terminal to the homeodomain, referred to as the CVC domain [for *ceh-10*, *Vsx-1* and *Chx10*, also referred to as the extended conservation region (Levine *et al.* 1994; Svendsen and McGhee 1995)]. The function of the CVC domain is not known.

As discussed above, the strong *ceh-10* alleles are likely to eliminate *ceh-10* function. In particular, the *ceh-10(gm133)* allele is a nonsense mutation that is predicted to terminate translation at the tenth amino acid of the homeodomain to produce a truncated protein with no DNA binding activity (Figure 5). The shared phenotypes of the other four strong mutants argue that they also completely lack *ceh-10* function. Two of these mutants, *gm58* and *gm71*, contain changes in amino acids that are conserved among the CEH-10, mouse Chx10 and goldfish Vsx-1 CVC domains, suggesting that the CVC domain is essential for function.

The gene *Chx10* specifies the fate of bipolar neurons of the retina. Chx10 is expressed in the neuroretina, the hindbrain and spinal cord, and its expression is maintained at high levels in bipolar cells of the retina (Liu *et al.* 1994). Ocular retardation (*or*) is a nonsense mutation in the *Chx10* gene that causes reduced proliferation of retinal progenitors and a lack of differentiated bipolar cells (Burmeister *et al.* 1996).

Like *Chx10*, we propose that *ceh-10* specifies the fate of neurons that express it. Both the CANs and AIY interneurons normally express the *ceh-10* and *ceh-23* genes (Wang *et al.* 1993; Svendsen and McGhee 1995). In strong *ceh-10* mutants, the CANs fail to migrate, and neither the CANs nor AIYs express *ceh-23-gfp* or *ceh-10-lacZ*. RMED neurons in *ceh-10* mutants no longer express detectable levels of their neurotransmitter GABA, suggesting that the fate of these cells has also been altered. Although we have not been able to unambiguously detect the RMED or displaced CAN neurons among the other neurons of the head ganglia, we have detected the AIY neuron in strong *ceh-10* mutants, indicating that AIY is produced, but fails to differentiate normally (see materials and methods). We also propose that some aspects of *ceh-10*-dependent differentiation of the CANs and AIY interneurons are regulated by CEH-23. Because *ceh-23* mutants have not been reported, we do not know how CEH-23 regulates CAN or AIY differentiation. By analogy to CEH-10, we propose that Chx10 might act through other transcriptional regulators to control bipolar cell fate.

Unlike complete loss-of-function mutants, CAN cells in partial loss-of-function *ceh-10* mutants express *ceh-23-gfp*, and migrate more than half their normal distance (Forrester and Garriga 1997). In these mutants, CAN cells must retain function, because a complete lack of CAN function is lethal.

Mutants that retain partial *ceh-10* activity exhibit CAN cell migration defects, but still express *ceh-23-gfp* in CANs and AIY, raising the possibility that *ceh-10* acts independently of *ceh-23* to regulate genes involved in cell migration. Alternatively, *ceh-10* could act through *ceh-23* to regulate cell migration genes, and *ceh-23* expression in weak *ceh-10* mutants would be insufficient to properly regulate genes that control CAN cell migration. Identification of transcriptional targets of the *ceh-10* and *ceh-23* homeodomain genes should provide insight into the mechanisms by which neurons acquire their unique migratory and functional properties.

We thank Cori Bargmann, Paul Baum, Scott Clark, David Baillie, Jim McGhee, Dianne Parry, Helen Stewart, Pia Svendsen and Theresa Stiernagle and the Caenorhabditis Genetics Center for providing strains. Some strains used in this work were provided by the *C. elegans* Genetic Toolkit Project, which is funded by a grant from the National Institutes of Health to Ann M. Rose, David L. Baillie and Donald L. Riddle. We thank Nancy Hawkins for critical reading of this manuscript and Claire Walczak for assistance with producing figures. This work was supported by National

Institutes of Health (NIH) grant NS-32057 to G.G., by postdoctoral fellowships from the NIH and from the Breast Cancer Research Program of the U.S. Army Medical Research and Materiel Command to W.C.F., and by a predoctoral fellowship from the National Science Foundation to J.A.Z.

LITERATURE CITED

Ackerman, S. L., L. P. Kozak, S. A. Przyborski, L. A. Rund, B. B. Boyer *et al.*, 1997 The mouse rostral cerebellar malformation gene encodes an UNC-5-like protein. Nature **386:** 838–842.

Anderson, P., and S. Brenner, 1984 A selection for myosin heavy chain mutants in the nematode *Caenorhabditis elegans.* Proc. Natl. Acad. Sci. USA **81:** 4470–4474.

Austin, J., and J. Kimble, 1989 Transcript analysis of *glp-1* and *lin-12,* homologous genes required for cell interactions during development of *C. elegans.* Cell **58:** 565–571.

Baum, P. D., and G. Garriga, 1997 Neuronal migrations and axon fasciculation are disrupted in *ina-1* integrin mutants. Neuron **19:** 51–62.

Bloom, L., and H. R. Horvitz, 1997 The *Caenorhabditis elegans* gene *unc-76* and its human homologs define a new gene family involved in axonal outgrowth and fasciculation. Proc. Natl. Acad. Sci. USA **94:** 3414–3419.

Brenner, S., 1974 The genetics of *Caenorhabditis elegans.* Genetics **77:** 71–94.

Burmeister, M., J. Novak, M. Y. LIang, S. Basu, L. Ploder *et al.*, 1996 Ocular retardation mouse caused by *Chx10* homeobox null allele: impaired retinal progenitor proliferation and bipolar cell differentiation. Nat. Genet. **12:** 376–384.

Cassada, R. C., and R. L. Russell, 1975 The dauerlarva, a post-embryonic developmental variant of the nematode *Caenorhabditis elegans.* Dev. Biol. **46:** 326–342.

Chalfie, M., J. N. Thomson and J. E. Sulston, 1983 Induction of neuronal branching in *Caenorhabditis elegans.* Science **221:** 61–63.

Chalfie, M., Y. Tu, G. Euskirchen, W. W. Ward and D. C. Prasher, 1994 Green fluorescent protein as a marker for gene expression. Science **263:** 802–805.

Chan, S. S., H. Zheng, M. W. Su, R. Wilk, M. T. Killeen *et al.*, 1996 UNC-40, a *C. elegans* homolog of DCC (deleted in colorectal cancer), is required in motile cells responding to UNC-6 netrin cues. Cell **87:** 187–195.

Chisholm, A., 1991 Control of cell fate in the tail region of *C. elegans* by the gene *egl-5.* Development **111:** 921–932.

Chisholm, A. D., and H. R. Horvitz, 1995 Patterning of the *Caenorhabditis elegans* head region by the Pax-6 family member *vab-3.* Nature **376:** 52–55.

Costa, M., M. Weir, A. Coulson, J. Sulston and C. Kenyon, 1988 Posterior pattern formation in *C. elegans* involves position-specific expression of a gene containing a homeobox. Cell **55:** 747–756.

DeLong, L., J. D. Plenefisch, R. D. Klein and B. J. Meyer, 1993 Feedback control of sex determination by dosage compensation revealed through *Caenorhabditis elegans sdc-3* mutations. Genetics **133:** 875–896.

Desai, C., G. Garriga, S. L. McIntire and H. R. Horvitz, 1988 A genetic pathway for the development of the *Caenorhabditis elegans* HSN motor neurons. Nature **336:** 638–646.

Fazeli, A., S. L. Dickinson, M. L. Hermiston, R. V. Tighe, R. G. Steen *et al.*, 1997 Phenotype of mice lacking functional Deleted in colorectal cancer (*Dcc*) gene. Nature **386:** 796–804.

Fire, A., S. W. Harrison and D. Dixon, 1990 modular set of *lacZ* fusion vectors for studying gene expression in *Caenorhabditis elegans.* Gene **93:** 189–198.

Forrester, W., and G. Garriga, 1997 Genes necessary for *C. elegans* cell and growth cone migrations. Development **124:** 1831–1843.

Garriga, G., C. Desai and H. R. Horvitz, 1993 Cell interactions control the direction of outgrowth, branching and fasciculation of the HSN axons of *Caenorhabditis elegans.* Development **117:** 1071–1087.

Golden, J. W., and D. L. Riddle, 1984 The *Caenorhabditis elegans* dauer larva: developmental effects of pheromone, food, and temperature. Dev. Biol. **102:** 368–378.

Greenwald, I. S., P. W. Sternberg and H. R. Horvitz, 1983 The *lin-12* locus specifies cell fates in *Caenorhabditis elegans.* Cell **34:** 435–444.

Harris, R., L. M. Sabatelli and M. A. Seeger, 1996 Guidance cues at the Drosophila CNS midline: identification and characterization of two Drosophila Netrin/UNC-6 homologs. Neuron **17:** 217–228.

Hawkins, N. C., and J. D. McGhee, 1990 Homeobox containing genes in the nematode *Caenorhabditis elegans.* Nucleic Acids Res. **18:** 6101–6106.

Hedgecock, E. M., J. G. Culotti and D. H. Hall, 1990 The *unc-5, unc-6* and *unc-40* genes guide circumferential migrations of pioneer axons and mesodermal cells on the epidermis in *C. elegans.* Neuron **4:** 61–85.

Hosono, R., K. Hirahara, S. Kuno and T. Kurihra, 1982 Mutants of *Caenorhabditis elegans* with dumpy and rounded head phenotype. J. Exp. Zool. **224:** 135–144.

Huang, L. S., P. Tzou and P. W. Sternberg, 1994 The *lin-15* locus encodes two negative regulators of *Caenorhabditis elegans* vulval development. Mol. Biol. Cell **5:** 395–411.

Keino, M. K., M. Masu, L. Hinck, E. D. Leonardo, S. S. Chan *et al.*, 1996 Deleted in *Colorectal Cancer* (DCC) encodes a netrin receptor. Cell **87:** 175–185.

Kenyon, C., 1986 A gene involved in the development of the posterior body region of *C. elegans.* Cell **46:** 477–487.

Kolodziej, P. A., L. C. Timpe, K. J. Mitchell, S. R. Fried, C. S. Goodman *et al.*, 1996 *frazzled* encodes a Drosophila member of the DCC immunoglobulin subfamily and is required for CNS and motor axon guidance. Cell **87:** 197–204.

Lander, A. D., 1989 Understanding the molecules of neural cell contacts: emerging patterns of structure and function. Trends Neurosci. **12:** 189–195.

Lauffenburger, D. A., and A. F. Horwitz, 1996 Cell migration: a physically integrated molecular process. Cell **84:** 359–369.

Leonardo, E. D., L. Hinck, M. Masu, M. K. Keino, S. L. Ackerman *et al.*, 1997 Vertebrate homologues of *C. elegans* UNC-5 are candidate netrin receptors. Nature **386:** 833–838.

Leung-Hagesteijn, C., A. M. Spence, B. D. Stern, Y. Zhou, M.-W. Su *et al.*, 1992 UNC-5, a transmembrane protein with immunoglobulin and thrombospondin type 1 domains, guides cell and pioneer axon migrations in *C. elegans.* Cell **71:** 289–299.

Levine, E. M., P. F. Hitchcock, E. Glasgow and N. Schechter, 1994 Restricted expression of a new paired-class homeobox gene in normal and regenerating adult goldfish retina. J. Comp. Neurol. **348:** 596–606.

Liu, I. S., J. D. Chen, L. Ploder, D. Vidgen, D. van der Kooy *et al.*, 1994 Developmental expression of a novel murine homeobox gene (*Chx10*): evidence for roles in determination of the neuroretina and inner nuclear layer. Neuron **13:** 377–393.

Luo, Y., and J. A. Raper, 1994 Inhibitory factors controlling growth cone motility and guidance. Curr. Opin. Neurobiol. **4:** 648–654.

Manser, J., and W. B. Wood, 1990 Mutations affecting embryonic cell migrations in *Caenorhabditis elegans.* Dev. Genet. **11:** 49–64.

Meneely, P. M., and R. K. Herman, 1979 Lethals, steriles and deficiencies in a region of the X chromosome of *Caenorhabditis elegans.* Genetics **92:** 99–115.

Mitchell, K. J., J. L. Doyle, T. Serafini, T. E. Kennedy, M. Tessier-Lavigne *et al.*, 1996 Genetic analysis of Netrin genes in Drosophila: Netrins guide CNS commissural axons and peripheral motor axons. Neuron **17:** 203–215.

Mitchison, T. J., and L. P. Cramer, 1996 Actin-based cell motility and cell locomotion. Cell **84:** 371–379.

Nobes, C. D., and A. Hall, 1995 Rho, rac, and cdc42 GTPases regulate the assembly of multimolecular focal complexes associated with actin stress fibers, lamellipodia, and filopodia. Cell **81:** 53–62.

Park, E. C., and H. R. Horvitz, 1986 Mutations with dominant effects on the behavior and morphology of the nematode *Caenorhabditis elegans.* Genetics **113:** 821–852.

Salser, S. J., and C. Kenyon, 1992 Activation of a *C. elegans* Antennapedia homologue in migrating cells controls their direction of migration. Nature **355:** 255–258.

Sambrook, J., E. F. Fritsch and T. Maniatis, 1989 *Molecular Cloning: A Laboratory Manual.* Cold Spring Harbor Laboratory Press, Cold Spring Harbor, NY.

Serafini, T., S. A. Colamarino, E. D. Leonardo, H. Wang, R. Bed-

dington *et al.*, 1996 Netrin-1 is required for commissural axon guidance in the developing vertebrate nervous system. Cell **87:** 1001–1014.

Serafini, T., T. E. Kennedy, M. J. Galko, C. Mirzayan, T. M. Jessell *et al.*, 1994 The netrins define a family of axon outgrowth-promoting proteins homologous to *C. elegans* UNC-6. Cell **78:** 409–424.

Sigurdson, D. C., G. J. Spanier and R. K. Herman, 1984 *Caenorhabditis elegans* deficiency mapping. Genetics **108:** 331–345.

Sulston, J. E., and H. R. Horvitz, 1977 Post-embryonic cell lineages of the nematode, *Caenorhabditis elegans*. Dev. Biol. **56:** 110–156.

Sulston, J. E., E. Schierenberg, J. G. White and J. N. Thomson, 1983 The embryonic lineage of the nematode *Caenorhabditis elegans*. Dev. Biol. **100:** 64–119.

Svendsen, P. C., and J. D. McGhee, 1995 The *C. elegans* neuronally expressed homeobox gene *ceh-10* is closely related to genes expressed in the vertebrate eye. Development **121:** 1253–1262.

Wadsworth, W. G., H. Bhatt and E. M. Hedgecock, 1996 Neuroglia and pioneer neurons express UNC-6 to provide global and local netrin cues for guiding migrations in *C. elegans*. Neuron **16:** 35–46.

Wang, B. B., I. M. Muller, J. Austin, N. T. Robinson, A. Chisholm *et al.*, 1993 A homeotic gene cluster patterns the anteroposterior body axis of *C. elegans*. Cell **74:** 29–42.

Waterston, R. H., J. N. Thomson and S. Brenner, 1980 Mutants with altered muscle structure of *Caenorhabditis elegans*. Dev. Biol. **77:** 271–302.

White, J. G., E. Southgate, J. N. Thomson and S. Brenner, 1986 The structure of the nervous system of *Caenorhabditis elegans*. Philos. Trans. R. Soc. Lond. B Biol. Sci. **314:** 1–340.

Wightman, B., S. G. Clark, A. M. Taskar, W. C. Forrester, A. V. Maricq *et al.*, 1996 The *C. elegans* gene *vab-8* guides posteriorly directed axon outgrowth and cell migration. Development **122:** 671–682.

Williams, B. D., B. Schrank, C. Huynh, R. Shownkeen and R. H. Waterston, 1992 A genetic mapping system in *Caenorhabditis elegans* based on polymorphic sequence-tagged sites. Genetics **131:** 609–624.

Zengel, J. M., and H. F. Epstein, 1980 Identification of genetic elements associated with muscle structure in the nematode *Caenorhabditis elegans*. Cell Motil. **1:** 73–97.

Communicating editor: I. Greenwald